

# Observation of Q-switching and mode-locking in two-section InAs-InP (100) quantum dot lasers at 1.53 $\mu\text{m}$

**Citation for published version (APA):**

Heck, M. J. R., Bente, E. A. J. M., Smalbrugge, E., Oei, Y. S., Smit, M. K., Anantathanasarn, S., & Nötzel, R. (2007). Observation of Q-switching and mode-locking in two-section InAs-InP (100) quantum dot lasers at 1.53  $\mu\text{m}$ . *Optics Express*, 15(25), 16292-16301. <https://doi.org/10.1364/OE.15.016292>

**DOI:**

[10.1364/OE.15.016292](https://doi.org/10.1364/OE.15.016292)

**Document status and date:**

Published: 01/01/2007

**Document Version:**

Publisher's PDF, also known as Version of Record (includes final page, issue and volume numbers)

**Please check the document version of this publication:**

- A submitted manuscript is the version of the article upon submission and before peer-review. There can be important differences between the submitted version and the official published version of record. People interested in the research are advised to contact the author for the final version of the publication, or visit the DOI to the publisher's website.
- The final author version and the galley proof are versions of the publication after peer review.
- The final published version features the final layout of the paper including the volume, issue and page numbers.

[Link to publication](#)

**General rights**

Copyright and moral rights for the publications made accessible in the public portal are retained by the authors and/or other copyright owners and it is a condition of accessing publications that users recognise and abide by the legal requirements associated with these rights.

- Users may download and print one copy of any publication from the public portal for the purpose of private study or research.
- You may not further distribute the material or use it for any profit-making activity or commercial gain
- You may freely distribute the URL identifying the publication in the public portal.

If the publication is distributed under the terms of Article 25fa of the Dutch Copyright Act, indicated by the "Taverne" license above, please follow below link for the End User Agreement:

[www.tue.nl/taverne](http://www.tue.nl/taverne)

**Take down policy**

If you believe that this document breaches copyright please contact us at:

[openaccess@tue.nl](mailto:openaccess@tue.nl)

providing details and we will investigate your claim.

# Observation of Q-switching and mode-locking in two-section InAs/InP (100) quantum dot lasers around 1.55 $\mu\text{m}$

Martijn J.R. Heck, Erwin A.J.M. Bente, Barry Smalbrugge, Yok-Siang Oei, Meint K. Smit, Sanguan Anantathanasarn and Richard Nötzel

COBRA Research Institute, Technische Universiteit Eindhoven, Den Dolech 2, 5600 MB Eindhoven, The Netherlands  
[m.heck@tue.nl](mailto:m.heck@tue.nl)

<http://www.cobra.tue.nl>

**Abstract:** First observation of passive mode-locking in two-section quantum-dot lasers operating at wavelengths around 1.55  $\mu\text{m}$  is reported. Pulse generation at 4.6 GHz from a 9 mm long device is verified by background-free autocorrelation, RF-spectra and real-time oscilloscope traces. The output pulses are stretched in time and heavily up-chirped with a value of 20 ps/nm, contrary to what is normally observed in passively mode-locked semiconductor lasers. The complete output spectrum is shown to be coherent over 10 nm. From a 7 mm long device Q-switching is observed over a large operating regime. The lasers have been realized using a fabrication technology that is compatible with further photonic integration. This makes the laser a promising candidate for e.g. a mode-comb generator in a complex photonic chip.

©2007 Optical Society of America

**OCIS codes:** (130.0250) Optoelectronics; (140.3540) Lasers, Q-switched; (140.4050) Mode-locked lasers; (140.5960) Semiconductor lasers; (250.5590) Quantum-well, -wire and -dot devices

---

## References and links

1. R. Kaiser, B. Hüttel, H. Heidrich, S. Fidorra, W. Rehbein, H. Stolpe, R. Stenzel, W. Ebert, and G. Sahin, "Tunable monolithic mode-locked lasers on InP with low timing jitter," *IEEE Photon. Technol. Lett.* **15**, 634–636 (2003).
2. R. Kaiser and B. Hüttel, "Monolithic 40-GHz mode-locked MQW DBR lasers for high-speed optical communication systems," *IEEE J. Sel. Top. Quantum Electron.* **13**, 125-135 (2007).
3. K.A. Williams, M.G. Thompson and I.H. White, "Long-wavelength monolithic mode-locked diode lasers," *New J. Phys.* **6**, 179 (2004).
4. C. Gosset, K. Merghem, A. Martinez, G. Moreau, G. Patriarche, G. Aubin, A. Ramdane, J. Landreau and F. Lelarge, "Subpicosecond pulse generation at 134 GHz using a quantum-dash-based Fabry-Perot laser emitting at 1.56  $\mu\text{m}$ ," *Appl. Phys. Lett.* **88**, 241105 (2006).
5. M.G. Thompson, A. Rae, R.L. Sellin, C. Marinelli, R.V. Penty, I.H. White, A.R. Kovsh, S.S. Mikhlin, D.A. Livshits and I.L. Krestnikov, "Subpicosecond high-power mode locking using flared waveguide monolithic quantum-dot lasers," *Appl. Phys. Lett.* **88**, 133119 (2006).
6. Y. Barbarin, S. Anantathanasarn, E.A.J.M. Bente, Y.S. Oei, M.K. Smit and R. Nötzel, "1.55- $\mu\text{m}$  range InAs-InP (100) quantum-dot Fabry-Pérot and ring lasers using narrow deeply etched ridge waveguides," *IEEE Photon. Technol. Lett.* **18**, 2644-2646 (2006).
7. E.U. Rafailov, M.A. Cataluna, W. Sibbett, N.D. Il'inskaya, Y.M. Zadiranov, A.E. Zhukov, V.M. Ustinov, D.A. Livshits, A.R. Kovsh and N.N. Ledentsov, "High-power picosecond and femtosecond pulse generation from a two-section mode-locked quantum-dot laser," *Appl. Phys. Lett.* **87**, 081107 (2005).
8. E.U. Rafailov, P. Loza-Alvarez, W. Sibbett, G.S. Sokolovskii, D.A. Livshits, A.E. Zhukov and V.M. Ustinov, "Amplification of femtosecond pulses by over 18 dB in a quantum-dot semiconductor optical amplifier," *IEEE Photon. Technol. Lett.* **15**, 1023-1025 (2003).
9. S. Anantathanasarn, R. Nötzel, P.J. van Veldhoven, F.W.M. van Otten, Y. Barbarin, G. Servanton, T. de Vries, E. Smalbrugge, E.J. Geluk, T.J. Eijkemans, E.A.J.M. Bente, Y.S. Oei, M.K. Smit and J.H. Wolter, "Lasing of wavelength-tunable (1.55  $\mu\text{m}$  region) InAs/InGaAsP/InP (100) quantum dots grown by metal organic vapor-phase epitaxy," *Appl. Phys. Lett.* **89**, 073115 (2006).

10. J.J.M. Binsma, M. van Geemert, F. Heinrichsdorff, T. van Dongen, R.G. Broeke and M.K. Smit, "MOVPE waveguide regrowth in InGaAsP/InP with extremely low butt joint loss," in *Proc. Symp. IEEE/LEOS Benelux Chapter* (2001), pp. 245-248.
11. Y. Barbarin, E.A.J.M. Bente, T. de Vries, J.H. den Besten, P.J. van Veldhoven, M.J.H. Sander-Jochem, E. Smalbrugge, F.W.M. van Otten, E.J. Geluk, M.J.R. Heck, X.J.M. Leijtens, J.G.M. van der Tol, F. Karouta, Y.S. Oei, R. Nötzel and M.K. Smit, "Butt-joint interfaces in InP/InGaAsP waveguides with very low reflectivity and low loss," in *Proc. Symp. IEEE/LEOS Benelux Chapter* (2005), pp. 89–92.
12. Y. Barbarin, E.A.J.M. Bente, M.J.R. Heck, Y.S. Oei, R. Nötzel and M.K. Smit, "Characterization of a 15 GHz integrated bulk InGaAsP passively modelocked ring laser at 1.53 $\mu\text{m}$ ," *Opt. Express* **14**, 9716-9727 (2006).
13. E.A. Viktorov, P. Mandel, A.G. Vladimirov and U. Bandelow, "Model for mode locking in quantum dot lasers," *Appl. Phys. Lett.* **88**, 201102 (2006).
14. E.A. Viktorov, P. Mandel, M. Kuntz, G. Fiol, D. Bimberg, A.G. Vladimirov and M. Wolfram, "Stability of the modelocking regime in quantum dot laser," in *Conference on Lasers and Electro-Optics Europe, CLEO* (2007), paper IG6.
15. U. Bandelow, M. Radziunas, A. Vladimirov, B. Hüttl and R. Kaiser, "40 GHz mode-locked semiconductor lasers: theory, simulations and experiment," *Opt. Quantum Electron.* **38**, 495-512 (2006).

## 1. Introduction

Active and passive mode-locking of laser diodes is a well-established technique for generating picosecond pulses at wavelengths around 1.55  $\mu\text{m}$  [1,2,3]. These wavelengths are of primary interest for telecommunication applications. The material of choice for fabricating these mode-locked laser diodes (MLLDs) is InP/InGaAsP, using either bulk or quantum well gain sections [3]. Recently passive mode-locking has also been observed in quantum-dash based lasers [4].

Quantum dot (QD) gain material is promising for applications in MLLDs due to the broad gain spectrum, low spontaneous emission levels and a low threshold current density [5,6]. In principle this allows for the generation of ultrashort, transform limited pulses. Sub-picosecond pulse generation down to 0.4 ps pulse duration has been achieved with InAs-GaAs QD material operating at wavelengths around 1.3  $\mu\text{m}$  [5,7]. Sub-picosecond pulse amplifiers [8] and MLLDs have been realized with this material demonstrating average output powers of 45 mW, with pulse peak powers over 1 W [7]. Recently we have reported lasing in Fabry-Pérot (FP) type ridge waveguide InAs/InP (100) QD structures operating in the 1.55  $\mu\text{m}$  wavelength region [9]. It was demonstrated that similarly to the InAs-GaAs QD material, this material does not suffer from ridge side-wall surface recombination. As a result it is possible to make high-contrast ridge waveguides, reducing the size of the devices and increasing the possible integration density [6].

In this work the first results obtained with monolithic two-section QD lasers operating at wavelengths around 1.55  $\mu\text{m}$  are presented. First the device design and fabrication are presented in section 2. Hereafter the experimental results are presented and discussed for the laser configurations showing Q-switching (section 3) and passive mode-locking (PML, section 4). The conclusions are summarized in section 5.

## 2. Design and fabrication

The QD laser structure is grown on n-type InP (100) substrates by metal-organic vapor-phase epitaxy (MOVPE), as presented in [6,9]. The QD wavelength is tuned into the 1.55  $\mu\text{m}$  region through insertion of ultrathin GaAs interlayers. In the active region five InAs QD layers are stacked, separated by 40-nm InGaAsP layers with a bandgap corresponding to a wavelength of 1.25  $\mu\text{m}$  (Q1.25). The QDs have a diameter of approximately 50 nm and a height of 4 nm – 7 nm. The QD layers are placed in the center of a Q1.25 InGaAsP optical waveguiding core layer which is in total 500 nm thick. The bottom cladding of this laser structure is a 500-nm thick n-InP buffer and the top cladding is a 1.5- $\mu\text{m}$  p-InP with a compositionally graded 300-nm p-InGaAs(P) top contact layer. Note that this layerstack is compatible with the butt-joint active-passive integration process as mentioned in [10,11] for possible further integration.

Two-section FP-type laser devices have been designed and realized with total lengths of 4 mm up to 9 mm and section ratios of 3% up to 30%, as shown in Fig. 1. The ridge waveguides have a width of 2  $\mu\text{m}$  and are etched 100 nm into the InGaAsP Q1.25 layer. To create electrical isolation between the two sections, the most highly doped part of the p-cladding layer is etched away. The waveguide and isolation sections are etched using an optimized  $\text{CH}_4/\text{H}_2$  two-step reactive-ion dry etch process. The structures are planarized and passivated using polyimide. Two evaporated Ti/Pt/Au metal pads contact the two sections to create two electrical contacts. Au-plating is used to increase the Au-thickness to over 1  $\mu\text{m}$  to ensure uniform injection current and to increase dissipation of the generated heat. The backside of the n-InP substrate is metallized to create a common ground contact for the two sections. The structures are cleaved to create the mirrors for the FP cavity.

The two-section devices are operated by forward biasing the longer gain section, creating a semiconductor optical amplifier (SOA) and by reversely biasing the shorter gain section, creating a saturable absorber (SA). The devices are mounted on a copper chuck, p-side up. In this work we focus our analysis on two devices, i.e. a device with a length of 7 mm and an SA section of 5% of the total length and a device with a length of 9 mm, with an SA section of 3%. In the following these devices are used to investigate Q-switching and mode-locking respectively.

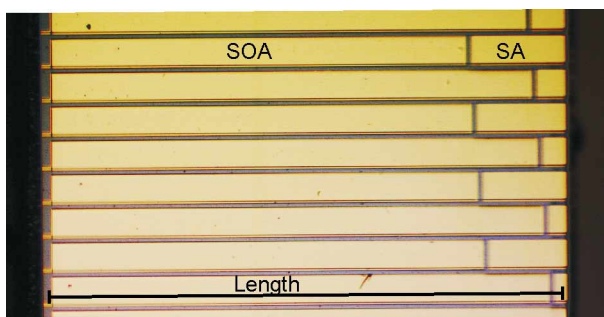


Fig. 1. Photograph of the realized devices, showing different configurations. The SOA (gain) and SA (saturable absorption) sections are indicated.

### 3. Q-switching

Q-switching of the laser by low-frequency (self-)modulation of the cavity losses, is a commonly found operating regime in two-section lasers, e.g. [12]. However in QD-based laser diodes, Q-switching is thought to be suppressed or even absent due to the fast recovery of the saturable gain [13,14].

Using the setup depicted in Fig. 2 a laser with a total length of 7 mm and an SA with a length of 5% of the total cavity (SA length equals 350  $\mu\text{m}$ ) is studied. Anti-reflection coated lensed fibers are used to couple light out of the laser and optical isolators are used to prevent feedback from reflections into the laser cavity. The copper chuck below the laser is kept at a fixed temperature of 10  $^{\circ}\text{C}$ . Needle probes are used to bias the two sections of the laser respectively.

In Fig. 3 the fiber-coupled output power is plotted as a function of the injection current. As can be seen, there is a step-like curve around the lasing threshold. This is because the SA saturates as a result of the increased optical power, resulting in a reduced optical loss. The lasing threshold current increases from around 700 mA for an SA voltage of 0 V, up to 775 mA with the bias voltage decreased to -3 V. These lasing thresholds are relatively large as compared to bulk or quantum-well lasers. The reason is the low modal gain of the QD lasers [9]. The reverse bias current is also recorded and it is observed to scale approximately with the intensity of the optical output. Moreover, sudden changes in optical power levels are observed when increasing the injection current, indicating dynamics in the optical field.

To study these dynamics the RF-spectrum of the laser is recorded, using a 50-GHz bandwidth electrical spectrum analyzer (ESA) with a 50-GHz photodiode. A reverse bias of

-3 V is applied. The RF-spectra for frequencies up to 5 GHz are plotted in Fig. 4(a). Three regimes of Q-switching can be identified, with RF-peak spacings of approximately 32.5 MHz, 153 MHz and 390 MHz with increasing injection current. The increase in the oscillation frequency with increasing injection current is in agreement with the observation in [14]. Q-switching has been verified by recording the optical output with a 6-GHz bandwidth oscilloscope and a 45-GHz photodiode. The traces are shown in Fig. 4(b) and are obtained with values for the injection current corresponding to the three regimes of Q-switching in Fig. 4(a). The pulse repetition rates corresponding to the RF-peak spacing are 31 ns, 6.5 ns and 2.6 ns respectively for increasing injection current. These repetition rates are in agreement with the oscilloscope traces in Fig. 4(b). The pulses are characterized by a steep (leading) peak, with a duration of 0.6 ps – 0.8 ps and a risetime of 0.3 ps. The pulses at 32.5 MHz and 153 MHz, i.e. at the lower injection currents, also have a significant trailing part, due to the relatively low gain just above threshold. Concluding we can say that passive Q-switching in QD-lasers has been shown.

A point to note is that the ESA spectra around 840 mA show no Q-switching, having an RF-peak around the cavity roundtrip time (outside the plot in Fig. 4(a)). This indicates a very small regime of possible mode-locking at this SA voltage value for this 7 mm device. Mode-locking in these two-section devices will be discussed in the next section for a 9 mm device. This regime around 840 mA corresponds to the peak in the *LI*-curve for the SA voltage of -3 V in Fig. 3.

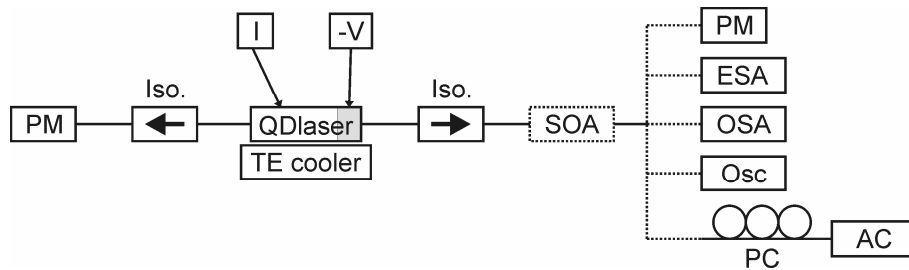


Fig. 2. Schematic overview of the setup used to characterize the QD lasers. PM: power meter, Iso: optical isolator, TE cooler: thermo-electric cooler, SOA: optional booster amplifier, ESA: electrical spectrum analyzer including a 50-GHz photodiode, OSA: optical spectrum analyzer, Osc: 6-GHz real time oscilloscope including 45-GHz photodiode, PC: polarization controller, AC: autocorrelator. All equipment is fiber pigtailed or has fiber input or output connectors. A current source (*I*) and voltage source (*-V*) are used to bias the SOA and SA respectively.

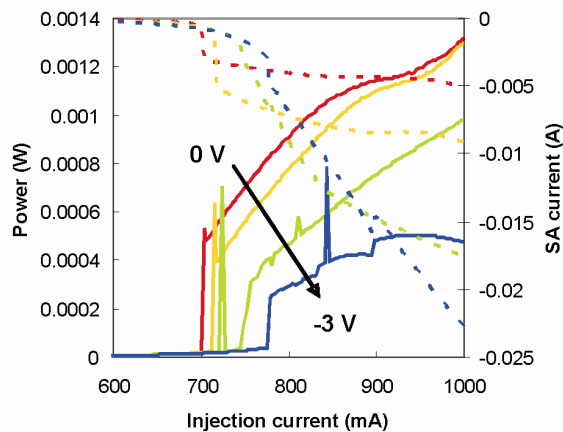


Fig. 3. *LI*-curves for different SA bias voltages (solid). The fiber coupled optical power is plotted. The SA bias current is also shown (dotted). The total device length is 7 mm and the SA length is 5%.

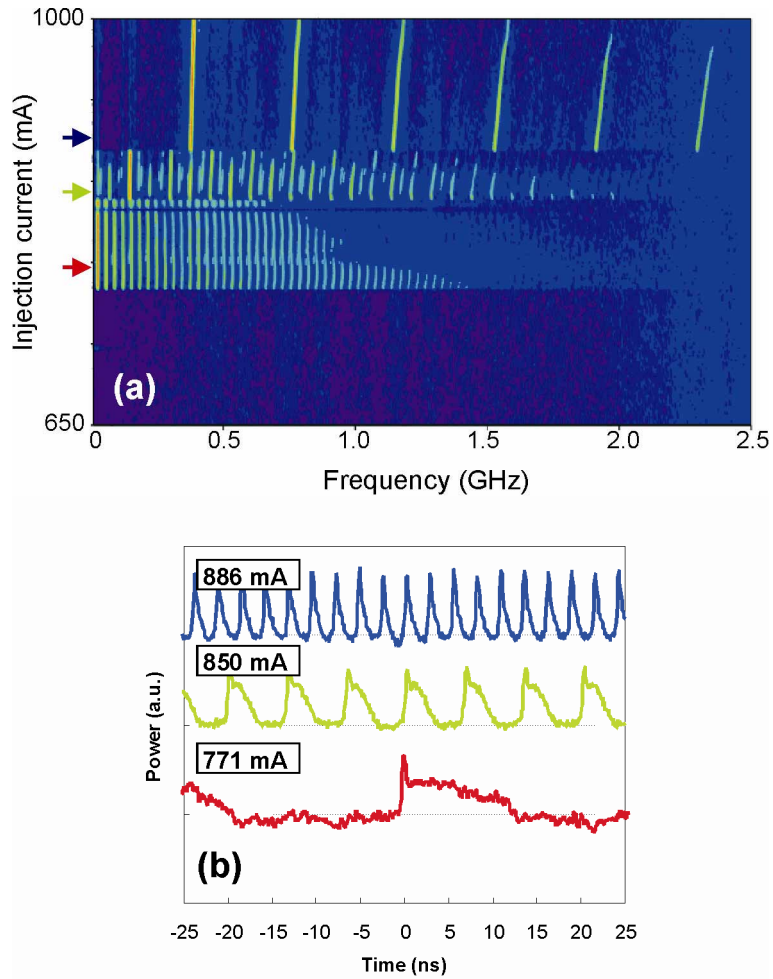


Fig. 4. (a) RF-spectra (3-MHz bandwidth resolution), color coded from low intensity (blue) to high intensity (red) obtained with a 7 mm device with 5% SA length and an SA bias voltage of -3 V. (b) Oscilloscope traces obtained for different injection currents corresponding to the three different regimes of Q-switching shown in (a) as indicated by the arrows. Traces have been offset for clarity, i.e. the dotted lines represent the respective 0-levels.

#### 4. Passive mode-locking

With the same setup as presented in Fig. 2 passive mode-locking in the QD-lasers is studied for a device with a total length of 9 mm and a 270  $\mu\text{m}$  (3%) SA section length. In Fig. 5 the *LI*-curves are given, showing threshold current values of 660 mA up to 690 mA for SA bias voltages of 0 V down to -4 V. Comparing these curves with the ones obtained for the 7 mm device in Fig. 3 it can be observed that threshold currents are lower for the 9 mm device and output power levels are of the same order. Moreover the step-like behavior around threshold is less pronounced owing to the shorter SA length.

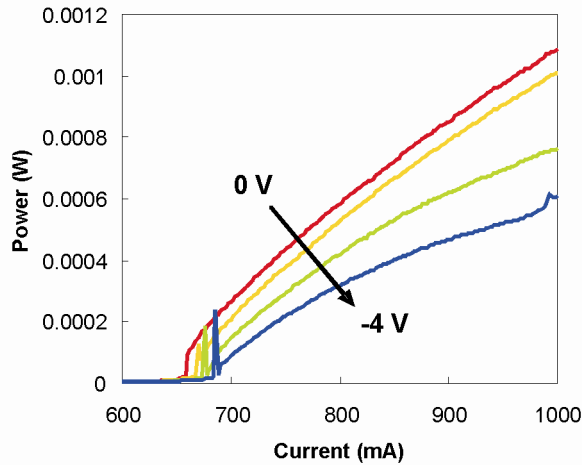


Fig. 5. *LI*-curves for different SA bias voltages. The fiber coupled optical power is plotted. The total device length is 9 mm and SA length is 3%.

The RF-spectra obtained for this laser show clear peaks at the cavity roundtrip-frequency of 4.6 GHz, corresponding to the 9-mm cavity. In Fig. 6 the RF-spectrum at an injection current of 900 mA and an SA bias voltage of -1 V is shown. The first RF-peak at the fundamental frequency is 43 dB over the noise floor. Also the width of this peak is narrow, i.e. 0.57 MHz at -20 dB, as can be seen in Fig. 6(b). Moreover, the lower-frequency signal intensity around the DC-component in the spectrum is very low, i.e. in the order of the noise floor up to 5 GHz. Concluding it can be said that this RF-spectrum indicates clear and stable mode-locking [15].

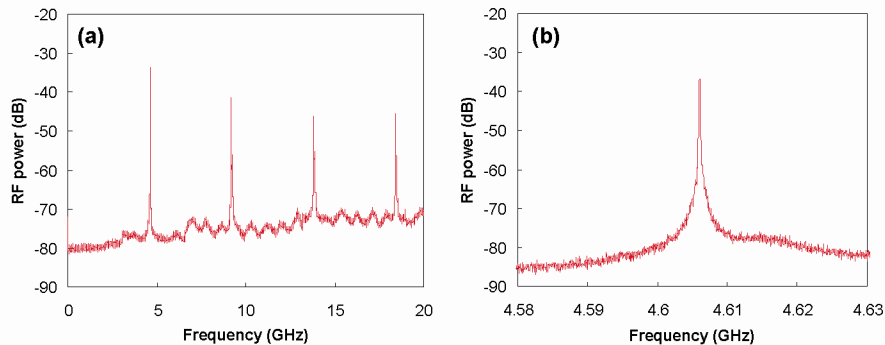


Fig. 6. (a) RF-spectrum obtained for a 9 mm device with 3% SA length. Injection current is 900 mA and SA bias voltage is -1 V. (b) Detailed view of the spectrum around the first RF-peak in (a). The electrical bandwidths used to obtain the spectra are 3 MHz and 50 kHz for (a) and (b) respectively.

The optical spectrum corresponding to this operating point is given in Fig. 7. Using an OSA with a 0.16-pm resolution, the mode-structure can clearly be distinguished, with a mode-spacing of 36 pm corresponding to the roundtrip frequency (Fig. 7(b)). The spectrum is broad, as can be expected from the inhomogeneously broadened gain of QD-lasers [5], but with a modulation on top (Fig. 7(a)), which is unlike to what is observed in a typical mode-locked spectrum of quantum-well or bulk gain lasers. However no clear pulse traces are obtained with the autocorrelator, using the setup as pictured in Fig. 2. Traces obtained with a 6-GHz bandwidth 10 Gs/s real-time oscilloscope showed a small modulation at 4.6 GHz, though with

a strong DC-offset. More specific, the modulation depth was only 15% of the total signal power.

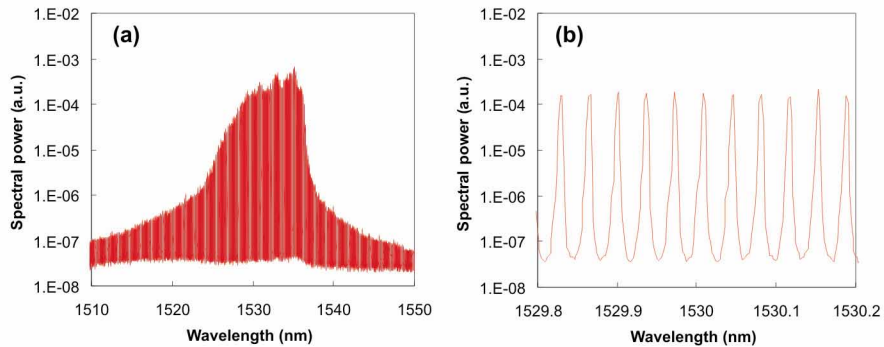


Fig. 7. (a) Optical spectrum obtained for a 9 mm device with 3% SA length. Injection current is 900 mA and SA bias voltage is -1 V. (b) Detailed view of the spectrum in (a). The optical bandwidth used to obtain the spectra is 0.16 pm.

To investigate the fact that the RF-spectrum shows a clear indication of mode-locking whereas there appears to be no significant pulse shaping, a tunable optical bandpass filter of 1.2 nm bandwidth is placed after the QD-laser output. A reduction of the DC component in the RF-spectrum, i.e. representing the average power, is observed (this DC component is not shown in Fig. 6(a)), while the RF-peaks at the fundamental frequency and their higher harmonics remain strong. Clear pulse shapes can now be observed with the autocorrelator, as can be seen in Fig. 8. With the filter set around 1534 nm, the width (FWHM) of the traces ranges from 9 ps up to 16 ps when increasing the injection current from 850 mA to 1.0 A. Assuming a deconvolution factor of 1.5 these values correspond to pulse durations of 6 ps to 11 ps. The traces are background-free, as they should be. Moreover the 6-GHz oscilloscope shows traces with a modulation depth down to the 0-Volt-level, i.e. background-free, as shown in the paragraphs below.

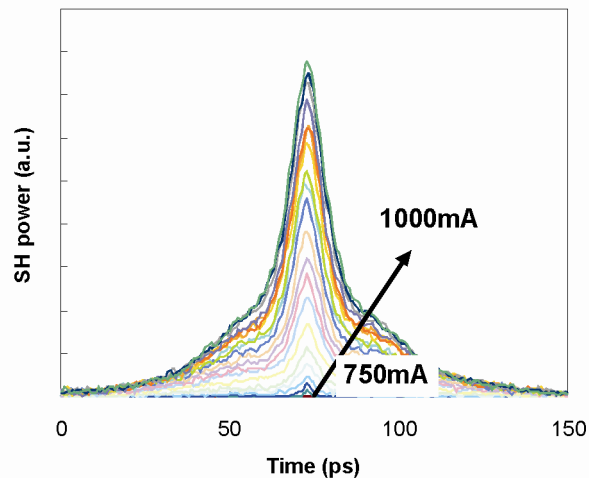


Fig. 8. Autocorrelator traces (second harmonic power given) obtained with a 9 mm device with 3% SA length and with a 1.2 nm optical bandpass filter. Injection current is varied from 750 mA up to 1.0 A and SA bias voltage is -1 V. A booster SOA is used for amplification.



By tuning the 1.2 nm bandpass filter over the full spectrum of the laser (approximately 10 nm as can be seen in Fig. 7), clearly defined picosecond pulses are observed at all wavelengths. Thus the laser is mode-locked over this range. To investigate the timing between these separate spectral components of the output pulse, the setup of Fig. 9 is used. Here the output pulses of the laser are split using a 3-dB coupler and they are separately filtered using two optical bandpass filters (with bandwidths of 1.2 nm and 2.0 nm respectively). Both filtered output pulses are then recorded with the 6-GHz oscilloscope. One of the bandpass filters (with 2.0 nm bandwidth) is kept at a fixed position and is used to trigger the signal, i.e. it serves as a reference. The other bandpass filter (with 1.2 nm bandwidth) is tuned and the output is recorded by the oscilloscope with the reference signal as a trigger. A typical oscilloscope trace is shown in Fig. 9(b).

Using these oscilloscope traces the relative delay of the pulse trains resulting after filtering is then determined. In Fig. 10 the optical spectra and resulting delays are plotted for different settings of the tunable bandpass filter. As can be seen the difference between the minimum and maximum delay is almost 0.2 ns, i.e. almost equal to the cavity roundtrip time of 216 ps. This leads to the conclusion that the output pulse of the QD-laser is very elongated, i.e. well over 100 ps duration, and is heavily up-chirped, with a chirp value of about 20 ps/nm. The chirp profile is predominantly linear over the pulse center as can be seen in Fig. 10(b). The full-bandwidth pulse duration of over 100 ps agrees with the 6 ps – 11 ps duration for the filtered pulse, assuming the chirp profile of Fig. 10(b). Note that the full bandwidth is coherent, effectively creating a mode-comb.

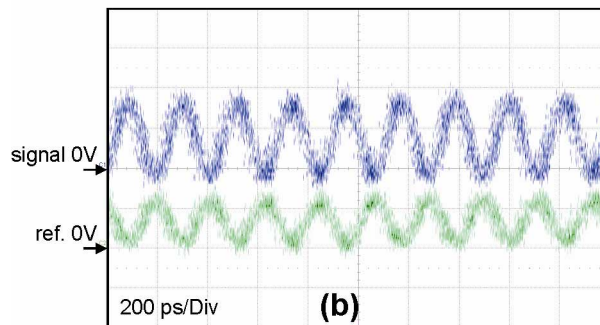
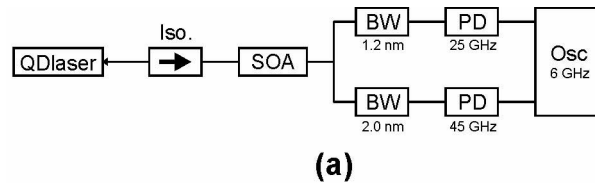


Fig. 9. (a) Schematic of the setup used to investigate the timing of the spectral components of the pulse. The two photodiodes (PDs) are connected to two channels of the oscilloscope (Osc). (b) A typical example of the oscilloscope traces. The 'signal' is obtained with the 1.2 nm filter and the 'ref.' with the 2.0 nm filter. The 'ref.' has a vertical offset for easy comparison.

The RF-peak at the fundamental frequency in the filtered laser output is stable, i.e. its value is stable within  $\pm 50$  kHz when the optical bandpass filter is tuned. This is demonstrated by measurement of the RF-spectra around this peak as a function of filter wavelength. A 0.3-nm wide tunable optical bandpass filter is used. The result is presented in Fig. 10(c), where the RF-spectra are shown over a 1.9 MHz frequency range. Tuning the position of the bandpass filter changes the intensity of the peak, much like the spectrum in Fig. 7(a), but not its position. However we have observed an increase in the pedestal around both the RF-peak and the DC-peak when the bandpass filter is included as compared to the case without a filter. This suggests that energy exchange between different spectral components of the pulse takes

place to some degree at lower frequencies, i.e. in the MHz-range. Investigation of this effect is beyond the scope of this work.

This result is strikingly different from what is commonly observed in mode-locked lasers based on bulk or quantum-well gain material, or even on QD gain material operating at wavelengths around 1.3  $\mu\text{m}$ , where shorter pulses with a lower time-bandwidth product are commonly obtained. The origin of the observed dynamics of the lasers presented here is not understood yet, however this will be investigated further by us. Most probably the laser behavior is related to the not well-known dynamics governed by the energy level structure and spectral inhomogeneous aspects in the 1.55  $\mu\text{m}$  QD gain material. For example as compared to the 1.3- $\mu\text{m}$  QD gain material our material has a relatively low carrier confinement in the dots and a relatively small energy separation between the ground and excited state due to the larger dot size.

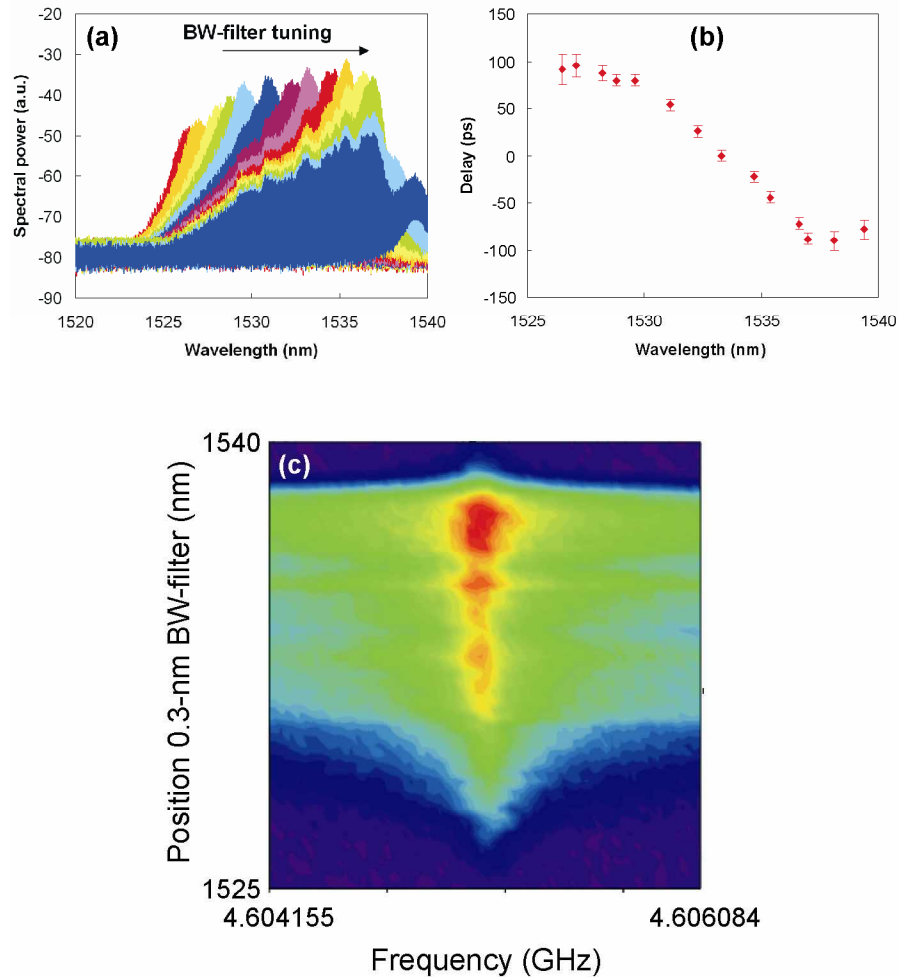


Fig. 10. (a) Resulting optical spectra by tuning the 1.2 nm optical bandpass filter. (b) Relative delay of the different pulse trains corresponding to the spectra in (a). (c) RF-spectra obtained after filtering the laser output with a 0.3-nm optical bandpass filter. Injection current is 1.0 A and SA bias voltage is -1 V. The spectra are color-coded in dB scale from low intensity (blue) to high intensity (red). The electrical bandwidth used to obtain the spectra is 50 kHz.

## 5. Conclusion

In this work mode-locking in two-section InAs/InP (100) QD-lasers operating at wavelengths around 1.55  $\mu\text{m}$  has been demonstrated for the first time. It has been verified by background-free autocorrelator signals, RF analyzer signals and real-time oscilloscope traces. The output pulses are heavily upchirped, with a value of 20 ps/nm. Pulse durations well over 100 ps are obtained for a repetition rate of 4.6 GHz. Mode-locking is very stable as indicated by the RF-peak power of 43 dB over the noise floor and a peak width of 0.57 MHz at -20 dB. The full optical bandwidth of the output is shown to be coherent. Moreover large regimes of Q-switching are observed in similar but slightly shorter devices and having a longer SA section with a higher bias voltage. As a result the saturation energy of the SA increases, leading to a decreased (or vanishing) regime of mode-locking.

These results indicate that the dynamics in our two-section InAs/InP (100) QD-lasers operating at 1.55  $\mu\text{m}$  are significantly different from their bulk and quantum-well counterparts and also from those published for 1.3  $\mu\text{m}$  InAs/GaAs QD-lasers.

Lasing thresholds in these devices are relatively high as compared to lasers based on bulk or quantum-well gain material and output power levels are relatively low because of the lower modal gain of the QD-lasers. This can in principle be improved by increasing the carrier confinement into the QDs by e.g. operation at a lower temperature or by decreasing the bandgap of the InGaAsP core layer. In the latter case the compatibility for possible further integration using an active-passive integration scheme [10,11] is compromised. Another more suitable option from point of view of integration, is to increase the number of QD-layers.

These devices have been realized with a fabrication technology that is compatible with further photonic integration. As such these devices can perform the function of e.g. a mode-comb generator in a complex photonic chip, and applications like an integrated arbitrary pulse shaper or spectral domain encoder become possible.

## Acknowledgements

This work was supported by the Netherlands Foundation of Scientific Research (NWO), the Dutch Technology Foundation STW through a Valorization Grant, and by the Dutch Ministry of Economic Affairs through the NRC Photonics Grant and the "Towards Freeband Communication Impulse" technology program.